Check for updates

# A highly selective fluorescence "turn-on" sensor for Ca²⁺ based on diarylethene with a triazozoyl hydrazine unit†

Zhen Wang, Shiqiang Cui, [ID] * Shouyu Qiu and Shouzhi Pu*

A new photochromic diarylethene derivative with a triazozoyl hydrazine unit has been designed and synthesized. Its photochromism and photoswitchable fluorescence behaviors were studied systematically by the stimuli of lights and chemical substances in acetonitrile solution. With the addition of Ca²⁺, the emission intensity enhanced 6.7 fold, accompanied by an obvious fluorescent color change from dark to light blue. The complexation between the derivative and Ca²⁺ is reversible with the 1 : 1 stoichiometry, which was verified by Job's plot and MS. The limit of detection (LOD) for Ca²⁺ was determined to be 2.49 × 10⁻⁸ mol L⁻¹. Based on this unimolecular platform, a logic circuit was designed with fluorescence intensity at 482 nm as the output and the combined stimuli of UV/vis and Ca²⁺/EDTA as four inputs.
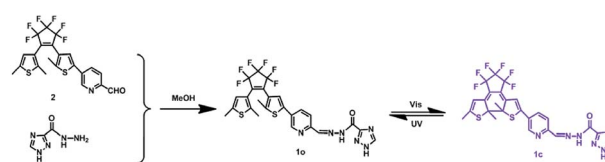
## Introduction

Calcium, the fifth most abundant element in the earth's crust, plays a very important role in many environmental and biological processes.[1–4] Meantime, Ca²⁺ is also a pivotal secondary messenger inside cells,[5–7] and visualization of Ca²⁺ intracellular dynamics has generated considerable biological knowledge.[8,9] Changes of Ca²⁺ concentration are related to immune responses and physiological responses to obesity.[10–17] High concentrations of Ca²⁺ ions will reduce the permeability of neuron membranes to sodium ions, thus reducing the excitability, resulting in low tension of smooth muscle.[18] Therefore, the effective and selective detection of Ca²⁺ ions is of great significance to medicine, environmental science and biochemistry.

Up to the present, there are a lot of traditional methods to detect various ions, such as atomic absorption spectrometry (AAS),[19] inductively coupled plasma mass spectrometry (ICP-MS),[20] voltammetry,[21] ion-selective membrane,[22] and liquid chromatography-mass spectrometry.[23] However, these methods all require high cost and complex instruments, and it is inconvenient to monitor the site quickly in different environments. Compared to these, a fluorescence probe is an effective tool to detect target ions due to its simplicity, easy implementation, high sensitivity and low detection limit.[24–31] To date, a number of fluorescent probes based on coumarin,[32] rhodamine,[33,34] nanoparticles,[35–37] polymeric phenols,[38,39] for the detection of Ca²⁺ have been reported. However, the Ca²⁺

selectivity of some probes is usually interfered by Mg²⁺ due to the similarly chemical behaviors of Ca²⁺ and Mg²⁺. What's more, few of the reported detection capabilities have fluorescent "on–off" mode for the detection of Ca²⁺ or its fluorescence enhancement rate is very small. Hence, developing novel fluorescence probes with higher sensitivity and selectivity for Ca²⁺ is of the utmost importance at present.

Among the reported fluorescence probes, diarylethene derivatives are the most promising candidates, due to their excellent thermal stability, remarkable fatigue resistance, drug resistance and rapid response.[40–42] Furthermore, the identified ions could induce the diarylethene molecular to undergo polystable conversion,[43] and these properties make it possible for the application in the filed of multi-addressable switching. Although some of processes have been made in diarylethenes based on ion recognition,[44–50] the sensors for Ca²⁺ ions based on diarylethenes have rarely been reported.[51,52]

In this article, a new Ca²⁺ fluorescent sensor (**1o**) based on diarylethene and the triazozoyl hydrazine unit was designed and synthesized. The structure of **1o** was characterized by ¹H NMR, ¹³C NMR, and HRMS, and the data were shown in ESI (Fig. S1–S3).† Its photochromism and fluorescent properties induced by lights and chemical species were also systematically discussed. The synthesis and photochromism of **1o** are shown in Scheme 1.

*Jiangxi Key Laboratory of Organic Chemistry, Jiangxi Science and Technology Normal University, Nanchang 330013, PR China. E-mail: cuisq2006@163.com; pushouzhi@tsinghua.org.cn; Fax: +86-791-83831996; Tel: +86-791-83831996*

Scheme 1 The synthetic route and photochromism of **1o**.

# Experimental

## General methods

Unless otherwise mentioned, all the reagents for the synthesis of the target compound were acquired from commercial suppliers and were used without further purification. All cations were added in the form of metal nitrates except for $K^+$, $Sn^{2+}$ and $Hg^{2+}$ (all of their counter ions were chloride ions). Metal ions solutions (0.1 mol $L^{-1}$) were prepared by dissolving their respective metal salts in deionized water. Necessary dilutions were made according to each experimental set up. NMR spectra were recorded on a Bruker AV400 spectrometer with deuterium generation of methanol (MeOD-$d_4$) and dimethylsulfoxide (DMSO-$d_6$) as solvents and tetramethylsilane (TMS) as an internal standard. Mass spectra were obtained using a Bruker Amazon SL ion trap mass spectrometer (ESI). The melting point was measured on a WRS-1B melting point apparatus. Absorption spectra were measured on an Agilent 8454 UV/vis spectrometer. Fluorescence spectra were recorded using a Hitachi F-4600 spectrophotometer. Photoirradiation was performed with an MUL-165 UV lamp and a MVL-210 visible lamp. Fluorescence quantum yield was measured with an Absolute PL Quantum Yield Spectrometer QYC11347-11.

## Synthesis of 1o

Diarylethene 1o was synthesized via the route shown in Scheme 1. Precursor 2 was synthesized according to the method reported in literature.[53] Then compound 2 (0.098 g, 0.2 mmol) was dissolved in 5.0 mL absolute methanol, followed by the addition of 1$H$-[1,2,4]triazole-3-carboxylic acid hydrazide (0.025 g, 0.2 mmol). The mixture was stirred for 12 h at room temperature in order to complete this reaction. After that, the solution was put into a refrigerator overnight. The crude product was washed with anhydrous methanol (5.0 mL × 3) and dried to give the bluish solid compound 1o (0.081 g, yield: 68%) with the mp of 488–490 K. $^1$H NMR (400 MHz, DMSO-$d_6$), δ (ppm): 1.86 (s, 3H), 1.95 (s, 3H), 2.41 (s, 3H), 6.84 (s, 1H), 7.72 (s, 1H), 8.00 (d, 1H, $J$ = 7.8 Hz), 8.15 (d, 1H, $J$ = 7.6 Hz), 8.60 (s, 1H), 8.81 (s, 1H), 8.90 (s, 1H), 12.35 (s, 1H), 14.70 (s, 1H). $^{13}$C NMR (100 MHz, CH$_3$OD-$d_4$), δ (ppm): 11.6, 11.8, 12.1, 119.8, 122.7, 123.0, 123.3, 125.0, 125.3, 128.1, 129.0, 132.0, 132.4, 136.3, 137.1, 138.6, 142.0, 144.0, 147.4, 150.7. HRMS: $m/z$ = 597.0943 [M + H$^+$]$^+$. Calcd 597.0968.

# Results and discussion

## Photochromism and fluorescent properties of 1o

The photochromic properties of 1o were studied in acetonitrile (2.0 × $10^{-5}$ mol $L^{-1}$) at room temperature as shown in Fig. 1A. The absorption maximum of 1o was observed at 343 nm ($\varepsilon$ = 4.4 × $10^4$ mol$^{-1}$ L cm$^{-1}$). Subsequently, upon irradiation with 297 nm light, a new broad absorption band centered at 572 nm ($\varepsilon$ = 1.2 × $10^4$ mol$^{-1}$ L cm$^{-1}$) emerged because of the formation of the closed-ring isomer 1c with larger π-electron delocalization in the molecule.[54] In the photostationary state (PSS), a clear isosbestic point was observed at 365 nm, accompanied by a distinct color change from colorless to purple, which

supported the reversible two-component photochromic reaction.[55] Conversely, upon irradiation with visible light ($\lambda$ > 500 nm), the colored solution of 1c was bleached entirely, and its absorption spectrum recovered to that of the open-ring isomer 1o. The quantum yields of cyclization and cycloreversion were determined to be 0.24 and 0.022, with 1,2-bis(2-methyl-5-phenyl-3-thienyl)perfluorocyclopentene as a reference.[56] Additionally, the photochromic cyclization/cycloreversion kinetics were studied in acetonitrile solution (2.0 × $10^{-5}$ mol $L^{-1}$) at room temperature. As described in Fig. S4A,† the relationships between the absorbance and exposure time have good linearity upon irradiation with 297 nm light, suggesting that the cyclization processes of 1o belong to the zeroth order reaction. The reaction rate constant ($k_{o-c}$) of 1o was determined to be 1.51 × $10^{-3}$ s$^{-1}$. Similarly, the relationship between −log(Abs) and exposure time also has perfect linearity, indicating that the cycloreversion process belong to the first order reaction. The reaction rate constant ($k_{c-o}$) was determined to be 4.39 × $10^{-2}$ s$^{-1}$ (Fig. S4B†). Furthermore, the fatigue resistance of 1o was also studied by alternating UV and visible lights at room temperature (Fig. S5†). The results indicated that the coloration–decoloration cycles between 1o and 1c could be repeated for 10 times with 15% degradation.

Fig. 1B showed the fluorescence spectral changes of 1o upon photoirradiation in acetonitrile solution (2.0 × $10^{-5}$ mol $L^{-1}$). The original state of 1o displayed weak fluorescence at 443 nm



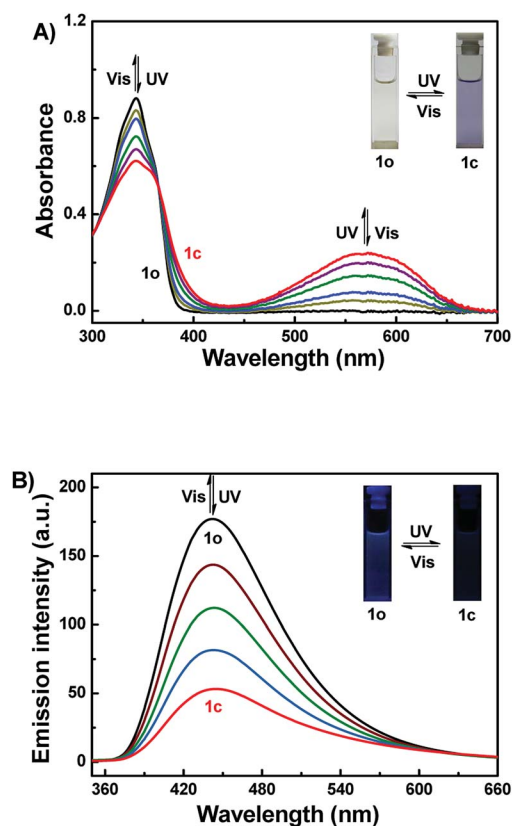Fig. 1 Changes in the absorption (A) and fluorescence (B) spectra of 1o upon irradiation with UV/vis lights in acetonitrile (2.0 × $10^{-5}$ mol L$^{-1}$) ($\lambda_{ex}$ = 340 nm).

when excited at 340 nm, and the absolute fluorescence quantum yield was determined to be 0.005. On irradiation with 297 nm light, its emission intensity at 443 nm decreased gradually due to the generation of non-fluorescent isomer **1c**. When the PSS was reached, the emission intensity of **1o** was decreased significantly by *ca.* 70%, accompanied by the fluorescence color changed from dark purple to dark. Back irradiation with the proper wavelength of visible light ($\lambda > 500$ nm) regenerated the open-ring isomer **1o** and recovered the original state.

### Fluorescence response to metal ions

Under the same experimental conditions, the fluorescence responses of **1o** toward various metal ions (5 equiv. 0.1 mol L$^{-1}$) were investigated in acetonitrile such as $Al^{3+}$, $Cu^{2+}$, $Sn^{2+}$, $Zn^{2+}$, $K^+$, $Ag^+$, $Ni^{2+}$, $Ba^{2+}$, $Mg^{2+}$, $Mn^{2+}$, $Cd^{2+}$, $Sr^{2+}$, $Hg^{2+}$, $Co^{2+}$, $Cr^{3+}$, $Fe^{3+}$, $Pb^{2+}$ and $Ca^{2+}$. As can be seen in Fig. 2, when $Ca^{2+}$ was added, the fluorescence intensity of **1o** was enhanced 6.7 fold as compared with the emission intensity of **1o** and the emission peak red shifted from 443 nm to 482 nm, accompanied by the fluorescent color change from dark purple to light blue. Furthermore, the fluorescence intensity of **1o** quenched with the addition of $Cu^{2+}$, $Co^{2+}$, $Ni^{2+}$. Moreover, upon addition of

other metal ions, including $Hg^{2+}$, $Mg^{2+}$, $Ca^{2+}$, $Ba^{2+}$, $Cr^{3+}$, $Al^{3+}$, $Mn^{2+}$, $Sr^{2+}$, $Pb^{2+}$, $Fe^{3+}$, and $K^+$, the fluorescence spectra of **1o** showed inconspicuous changes. All the results indicated that the excellent capability of **1o** for distinguishing $Ca^{2+}$ from other metals ions. Therefore, the diarylethene **1o** could be used as a selective fluorescence sensor for $Ca^{2+}$ in acetonitrile.

### Fluorescence studies of 1o toward Ca$^{2+}$

To further assess the responsive nature of **1o** induced by $Ca^{2+}$, the fluorescence spectral responses of **1o** toward $Ca^{2+}$ in acetonitrile were investigated in Fig. 3A. The results turned out that sensor **1o** exhibited a very weak emission with a low quantum yield ($\Phi = 0.005$) at 340 nm excitation. With the gradual addition of $Ca^{2+}$, the emission intensity dramatically increased by 6.7 fold, accompanied by a red shift of 39 nm from 443 nm to 482 nm. Then the fluorescence intensity achieved its maximum until the amount of $Ca^{2+}$ reached 2.2 equivalents of **1o** (Fig. S4†), and the absolute quantum yield of fluorescence was determined to be 0.03, which is 6 fold of **1o**. Meanwhile, the fluorescent color changed from dark purple to light blue, which was coincident with the changes in the fluorescence spectra. The weak fluorescence of the initial state **1o** was put down to the C=N isomerization, which has long been known as the dominant decay process.[57,58] However, a stable chelate **1o**–$Ca^{2+}$ was
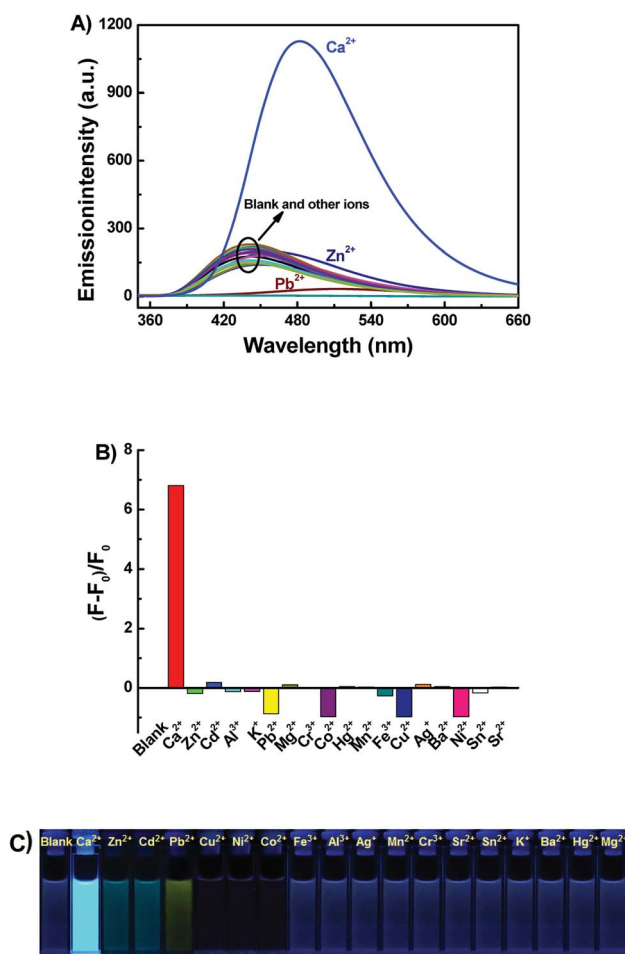


Fig. 2  Upon addition various metal ions to **1o** (2.0 × 10$^{-5}$ mol L$^{-1}$) in acetonitrile: (A) fluorescence emission spectral changes ($\lambda_{ex} = 340$ nm); (B) emission intensity changes; (C) fluorescent photos.
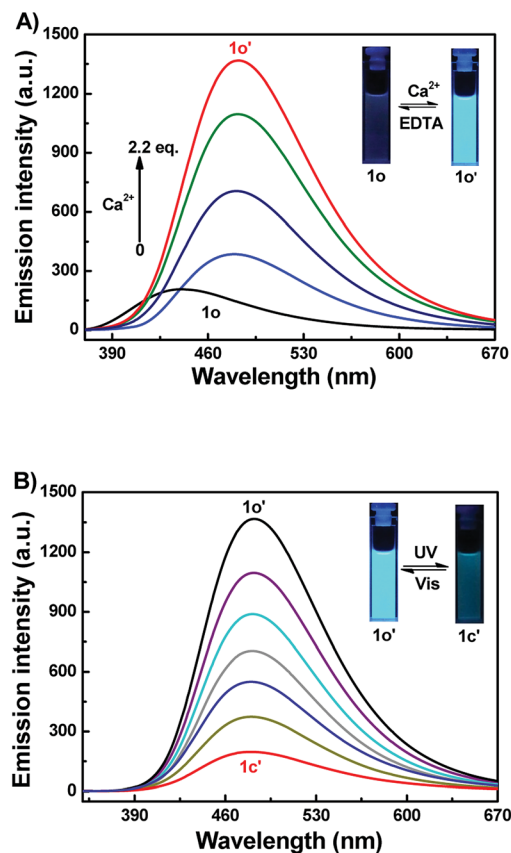


Fig. 3  (A) Fluorescence spectra changes of **1o** (2.0 × 10$^{-5}$ mol L$^{-1}$) in acetonitrile induced by $Ca^{2+}$ (0–2.2 equiv.); (B) fluorescence spectra changes of **1o′** (2.0 × 10$^{-5}$ mol L$^{-1}$ in acetonitrile), upon irradiation with UV-vis light ($\lambda_{ex} = 340$ nm).

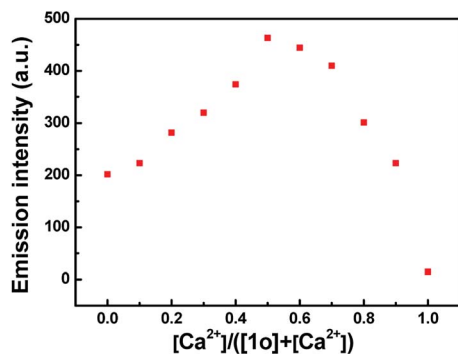**Fig. 4** Job's plot showing the 1 : 1 complex of **1o** and $Ca^{2+}$ in acetonitrile ($2.0 \times 10^{-5}$ mol $L^{-1}$).



**Scheme 2** Dual-controlled fluorescent switching behaviors of **1o** induced by $Ca^{2+}$/EDTA and UV/vis light.

formed with the existence of $Ca^{2+}$. The isomerization of C=N bond was inhibited, which enhanced the rigidity of the molecule, thus leading to the chelation enhanced fluorescence (CHEF) effect.[59] Furthermore, the reversibility experiment was established by adding 6.0 equiv. EDTA (0.1 mol $L^{-1}$) to **1o**–$Ca^{2+}$ (**1o′**) solution which possibly deprives $Ca^{2+}$ away from the binding position. Eventually, the fluorescence spectrum of **1o′** was brought back to that of **1o**, suggesting that the complexation–decomplexation reaction between **1o** and $Ca^{2+}$ was reversible.

### Complexation mechanism of 1o with $Ca^{2+}$

To further investigate the coordination mode of **1o** and $Ca^{2+}$, Job's plot analysis was performed by using the emission intensity at 482 nm for $Ca^{2+}$ as a function of molar fraction of **1o** according to the reported method.[60] As shown in Fig. 4, the maximum value was achieved when the molar fraction of $[Ca^{2+}]/([1o] + [Ca^{2+}])$ was about 0.5, suggesting that **1o** was bound to $Ca^{2+}$ with a 1 : 1 stoichiometry in acetonitrile. Based on these results and fluorescence titration data, the association constant ($K_a$) of **1o** with $Ca^{2+}$ was calculated from the slope and intercept of these linear plots to be $8.86 \times 10^3$ L $mol^{-1}$ with a good linear relationship ($R = 0.990$) (Fig. S6†). According to the method reported in previous literature,[61] the limit of detection (LOD) of **1o** toward $Ca^{2+}$ was determined to be $2.49 \times 10^{-8}$ mol $L^{-1}$ (Fig. S7†). Therefore, **1o** could serve as a fluorescent sensor for detection of $Ca^{2+}$ with high selectivity and sensitivity in acetonitrile.

$^{1}$H NMR titration experiments were also carried out in DMSO-$d_6$ to further study the binding mode of **1o** and $Ca^{2+}$. As shown in Fig. 5, the signals of the Ha (imino proton) at 12.48 ppm and the
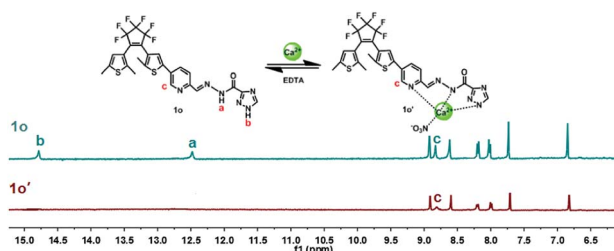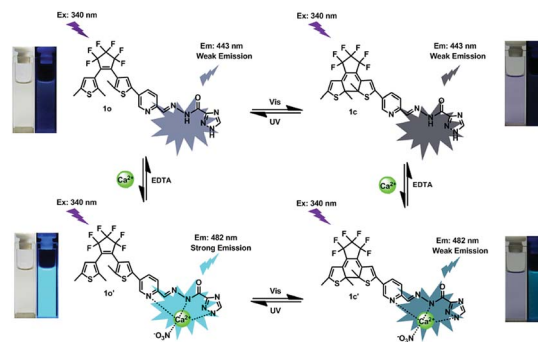
Hb (–NH– proton on the triazole) at 14.70 ppm were found in the $^{1}$H NMR spectrum of **1o**. With the addition of $Ca^{2+}$, the imino proton (Ha) disappeared completely, indicating the coordinate bond between imino N and $Ca^{2+}$ was formed. Meanwhile, the –NH– proton (Hb) on the triazole was also disappeared finally, indicating that the formation of coordinate bond between the N atom on the triazole and $Ca^{2+}$. On the other hand, the signal of Hc on CH=N decreased gradually, and the Hc displayed a downfield shift of 0.01 ppm from 8.81 ppm to 8.82 ppm ultimately, showing that the formation of the coordinate bond between the N atom on the Schiff base and $Ca^{2+}$. All of the results suggested that the imino N, the N on the Schiff base unit, and the N on the triazole ring are the most reasonable binding sites. Furthermore, the HRMS analysis was also carried out to confirm the interaction between **1o**–$Ca^{2+}$. The testing sample was prepared by adding excessive $Ca^{2+}$ to **1o** in acetonitrile, and the result displayed that the signal located at $m/z = 698.0362$ was consistent with the ensemble $[1o + Ca^{2+} + NO_3^-]^+$ ($m/z$ calcd: 698.0392) (Fig. S8†). These results further proved that **1o** and $Ca^{2+}$ formed a 1 : 1 complex. Based on these facts, the most likely binding mode was shown in Scheme 2. Furthermore, the affection of pH to the sensor was also investigated. According to the methods in our previous work,[62] the fluorescence intensity changes of **1o** and **1o′** over different pH values in $CH_3CN : H_2O$ (9 : 1, v/v) were shown in Fig. S11.† The results demonstrated that the optimal pH region for sensor **1o** and **1o′** was 6.0–9.0.

### Application in logic circuit and practical sample

According to the properties described above, the fluorescence emission of **1o** could be effectively modulated by either UV-vis



**Fig. 5** Changes in $^{1}$H NMR of **1o** and **1o′** in DMSO-$d_6$ (inset shows the proposed binding mode of **1o′** complex).
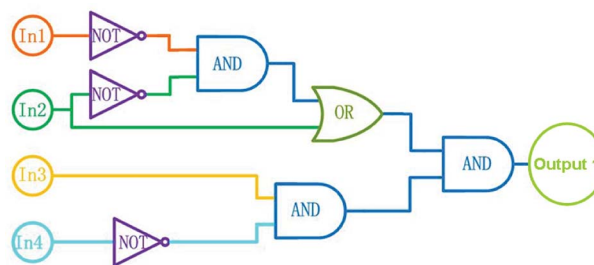


**Fig. 6** Combinational logic circuits equivalent to the truth table given in Table 1: In1 (UV light), In2 (visible light), In3 ($Ca^{2+}$), In4 (EDTA).

**Table 1** Truth table for all the possible strings of four binary-input data and the corresponding output digit

| Inputs | | | | Output[a] |
|---|---|---|---|---|
| In1 (UV) | In2 (Vis) | In3 ($Ca^{2+}$) | In4 (EDTA) | ($\lambda_{em}$ = 482 nm) |
| 0 | 0 | 0 | 0 | 0 |
| 1 | 0 | 0 | 0 | 0 |
| 0 | 1 | 0 | 0 | 0 |
| 0 | 0 | 1 | 0 | 1 |
| 0 | 0 | 0 | 1 | 0 |
| 1 | 1 | 0 | 0 | 0 |
| 1 | 0 | 1 | 0 | 0 |
| 1 | 0 | 0 | 1 | 0 |
| 0 | 1 | 1 | 0 | 1 |
| 0 | 1 | 0 | 1 | 0 |
| 0 | 0 | 1 | 1 | 0 |
| 1 | 1 | 1 | 0 | 1 |
| 1 | 1 | 0 | 1 | 0 |
| 1 | 0 | 1 | 1 | 0 |
| 0 | 1 | 1 | 1 | 0 |
| 1 | 1 | 1 | 1 | 0 |

[a] At 482 nm, the emission intensity 6.7 fold of the original value is defined as 1, otherwise defined as 0.

lights or chemical reagents stimuli in acetonitrile, and the photoswitching behaviors of **1o** are shown in Scheme 2. On the basis of these facts, a logic circuit was constructed by using UV (In1), vis (In2), $Ca^{2+}$ (In3), and EDTA (In4) as four input signals, and the emission intensity at 482 nm as the output signal (Fig. 6). The emission intensity of **1o** at 443 nm was considered as the initial value. When the emission intensity at 482 nm was 6.7 fold larger than the initial value, the output signal could serve as 'on' with a Boolean value of '1'. Otherwise, it serves as 'off' with a Boolean value of '0'. For instance, when the input strings were '1, 1, 1, and 0', the corresponding signals to In1, In2, In3, and In4 are 'on, on, on, and off'. Under this condition, **1o** was converted to **1o'** with the stimuli of $Ca^{2+}$, and the emission intensity increased dramatically. As a result, the output digital was '1'. Similarly, others stimuli would cause different on–off fluorescence switching. All of the possible logic strings were listed in the combinational logic circuit as shown in Table 1.

The application of **1o** to the practical samples was also performed. The $Ca^{2+}$ content in real water samples from the Ganjiang River in Nanchang, Jiangxi province were determined. Table 2 displayed the results measured with **1o** after adding a moderate amount of $Ca^{2+}$. The recovery was ranged from 96.8% to 105%. These results indicated that **1o** could be used for detecting $Ca^{2+}$ in practical samples with higher accuracy, and has certain practical value.

## Conclusions

In conclusion, a novel fluorescent sensor based on a diarylethene derivative with triazozoyl hydrazine unit was developed. The sensor exhibited high selectivity toward $Ca^{2+}$ over other metal ions, and the detection limit for $Ca^{2+}$ could be as low as $2.49 \times 10^{-8}$ mol $L^{-1}$. Furthermore, a logic circuit was designed and constructed with the emission intensity at 482 nm as output signal and the UV/vis lights, $Ca^{2+}$/EDTA as input signals. The application results indicated that the sensor could be used for the detection of $Ca^{2+}$ in practical samples. All these results will be helpful for the design and construction of new sensors for $Ca^{2+}$ with high selectivity and sensitivity in the future.

## Conflicts of interest

There are no conflicts to declare.

## Acknowledgements

## Notes and references

1 M. Landoni, B. F. Cerino, N. Haman, et al., J. Agric. Food Chem., 2013, **61**, 4622–4630.
2 S. M. Bawin and W. R. Adey, Proc. Natl. Acad. Sci. U. S. A., 1976, **73**, 1999–2003.
3 S. V. Dorozhkin and M. Epple, Angew. Chem., Int. Ed., 2002, **41**, 3130–3146.
4 S. Orrenius, B. Zhivotovsky and P. Nicotera, Nat. Rev. Mol. Cell Biol., 2003, **4**, 552.
5 D. E. Clapham, Cell, 2007, **131**, 1047–1058.
6 E. Arunkumar, A. Ajayaghosh and J. Daub, J. Am. Chem. Soc., 2005, **127**, 3156–3164.
7 T. Alizadeh, A. N. Shamkhali, Y. Hanifehpour, et al., New J. Chem., 2016, **40**, 8479–8487.
8 M. Raju, R. R. Nair, I. H. Raval, et al., Analyst, 2015, **140**, 7799–7809.
9 Y. Nakagawa, Y. Watanabe, Y. Igarashi, et al., Bioorg. Med. Chem. Lett., 2015, **25**, 2963–2966.
10 A. T. Harootunian, J. P. Kao, S. Paranjape, et al., Science, 1991, **251**, 75–78.
11 A. Minta, J. P. Kao and R. Y. Tsien, J. Biol. Chem., 1989, **264**, 8171–8178.

**Table 2** Application in practical samples detection for $Ca^{2+}$

| Sample | $Ca^{2+}$ added (μM) | $Ca^{2+}$ determined (μM) | Recovery (%) |
|---|---|---|---|
| 1 | 0.40 | 0.42 | 105 |
| 2 | 0.80 | 0.81 | 101 |
| 3 | 1.20 | 1.18 | 98.3 |
| 4 | 1.60 | 1.55 | 96.8 |
| 5 | 2.00 | 1.97 | 98.5 |

12 G. Grynkiewicz, M. Poenie and R. Y. Tsien, *J. Biol. Chem.*, 1985, **260**, 3440–3450.

13 K. V. Kuchibhotla, C. R. Lattarulo, B. T. Hyman, *et al.*, *Science*, 2009, **323**, 1211–1215.

14 I. Micu, A. Ridsdale, L. Zhang, *et al.*, *Nat. Med.*, 2007, **13**, 874.

15 D. Skokos, G. Shakhar, R. Varma, *et al.*, *Nat. Immunol.*, 2007, **8**, 835.

16 J. Chambers, R. S. Ames, D. Bergsma, *et al.*, *Nature*, 1999, **400**, 261.

17 C. M. Armstrong and G. Cota, *Proc. Natl. Acad. Sci. U. S. A.*, 1999, **96**, 4154–4157.

18 M. Frankowski, A. Zioła-Frankowska and J. Siepak, *Talanta*, 2010, **80**, 2120–2126.

19 A. Sanz-Medel, A. B. S. Cabezuelo, R. Milačič, *et al.*, *Coord. Chem. Rev.*, 2002, **228**, 373–383.

20 R. N. Goyal, V. K. Gupta and S. Chatterjee, *Biosens. Bioelectron.*, 2009, **24**, 3562–3568.

21 V. K. Gupta, A. K. Singh, S. Mehtab, *et al.*, *Anal. Chim. Acta*, 2006, **566**, 5–10.

22 V. K. Gupta, R. Jain, S. Sharma, *et al.*, *Int. J. Electrochem. Sci.*, 2012, 7, 569–587.

23 H. N. Kim, W. X. Ren, J. S. Kim, *et al.*, *Chem. Soc. Rev.*, 2012, **41**, 3210–3244.

24 Z. Shi, Y. Tu and S. Z. Pu, *RSC Adv.*, 2018, **8**, 6727–6732.

25 Y. L. Pak, K. M. K. Swamy and J. Yoon, *Sensors*, 2015, **15**, 24374–24396.

26 S. Pan, H. Tang, Z. Song, *et al.*, *Chin. J. Chem.*, 2017, **35**, 1263–1269.

27 M. Morimoto, Y. Takagi, K. Hioki, *et al.*, *Dyes Pigm.*, 2018, **153**, 144–149.

28 N. S. Wang, R. J. Wang, Y. Y. Tu, *et al.*, *Spectrochim. Acta, Part A*, 2018, **196**, 303–310.

29 N. Tetsuya, Y. Miyasaka and Y. Yokoyama, *Chem. Commun.*, 2018, **54**, 3207–3210.

30 C. Yu, L. Chen, J. Zhang, *et al.*, *Talanta*, 2011, **85**, 1627–1633.

31 C. Yu, J. Zhang, J. Li, *et al.*, *Microchim. Acta*, 2011, **174**, 247–255.

32 L. Cao, C. Jia, Y. Huang, *et al.*, *Tetrahedron Lett.*, 2014, **55**, 4062–4066.

33 X. Yu, P. Zhang, Q. Liu, *et al.*, *Mater. Sci. Eng., C*, 2014, **39**, 73–77.

34 M. S. Eom, W. Jang, Y. S. Lee, *et al.*, *Chem. Commun.*, 2012, **48**, 5566–5568.

35 J. Zhang, Y. Wang, X. Xu, *et al.*, *Analyst*, 2011, **136**, 3865–3868.

36 A. Ajayaghosh, E. Arunkumar and J. Daub, *Angew. Chem.*, 2002, **114**, 1844–1847.

37 S. K. Sharma, S. Kumar, R. Tyagi, *et al.*, *Microchem. J.*, 2008, **90**, 89–92.

38 R. Sahli, N. Raouafi, E. Maisonhaute, *et al.*, *Electrochim. Acta*, 2012, **63**, 228–231.

39 S. Z. Pu, T. S. Yang, J. K. Xu, *et al.*, *Tetrahedron*, 2005, **61**, 6623–6629.

40 S. Z. Pu, J. K. Xu, L. Shen, *et al.*, *Tetrahedron Lett.*, 2005, **46**, 871–875.

41 R. J. Wang, P. P. Ren, S. Z. Pu, *et al.*, *J. Photochem. Photobiol., A*, 2014, **294**, 44–53.

42 H. Tian, B. Qin, R. Yao, *et al.*, *Adv. Mater.*, 2003, **15**, 2104–2107.

43 Q. Zou, X. Li, J. Zhang, *et al.*, *Chem. Commun.*, 2012, **48**, 2095–2097.

44 A. Bianco, S. Perissinotto, M. Garbugli, *et al.*, *Laser Photonics Rev.*, 2011, **5**, 711–736.

45 Q. Zou, J. Jin, B. Xu, *et al.*, *Tetrahedron*, 2011, **67**, 915–921.

46 Z. Zhou, H. Yang, M. Shi, *et al.*, *ChemPhysChem*, 2007, **8**, 1289–1292.

47 Z. Zhou, S. Xiao, J. Xu, *et al.*, *Org. Lett.*, 2006, **8**, 3911–3914.

48 Z. Li, C. Zhang, Y. Ren, *et al.*, *Org. Lett.*, 2011, **13**, 6022–6025.

49 S. Z. Pu, D. Jiang, W. Liu, *et al.*, *J. Mater. Chem.*, 2012, **22**, 3517–3526.

50 R. Wang, X. Dong, G. Liu, *et al.*, *Luminescence*, 2015, **30**, 1290–1296.

51 S. Q. Cui, Z. Y. Tian, S. Z. Pu, *et al.*, *RSC Adv.*, 2016, **6**, 19957–19963.

52 S. Z. Pu, Z. P. Tong, G. Liu, *et al.*, *J. Mater. Chem. C*, 2013, **1**, 4726–4739.

53 M. Irie, *Chem. Rev.*, 2000, **100**, 1685–1716.

54 Z. X. Li, L. Y. Liao, W. Sun, *et al.*, *J. Phys. Chem. C*, 2008, **112**, 5190–5196.

55 S. Z. Pu, T. Yang, J. Xu, *et al.*, *Tetrahedron*, 2005, **61**, 6623–6629.

56 M. Irie, T. Lifka, S. Kobatake and N. Kato, *J. Am. Chem. Soc.*, 2000, **122**, 4871–4876.

57 W. K. Dong, X. L. Li, L. Wang, *et al.*, *Sens. Actuators, B*, 2016, **229**, 370–378.

58 E. T. Feng, Y. Y. Tu, C. B. Fan, *et al.*, *RSC Adv.*, 2017, **7**, 50188–50194.

59 Y. M. Xue, R. J. Wang, C. H. Zheng, *et al.*, *Tetrahedron Lett.*, 2016, **57**, 1877–1881.

60 W. Liu, L. Xu, R. Sheng, *et al.*, *Org. Lett.*, 2007, **9**, 3829–3832.

61 S. Guo, G. Liu, C. Fan, *et al.*, *Sens. Actuators, B*, 2018, **266**, 603–613.

62 Z. Wang, S. Q. Cui, S. Y. Qiu and S. Z. Pu, *Spectrochim. Acta, A*, 2018, **205**, 21–28.